Vector and siRNA for CD55

CD55 cDNA in Ultimate open reading frame (ORF) clones (clone *ID*: IOH3209) was purchased from Invitrogen, and amplified by polymerase chain reaction (PCR) (forward, 5′-CGCGGATCCGCGATGACCGTCGCGCGG-3′; and reverse, 5′-TCCCCCGGGGGACTAAGTCAGCAAGCC-3′). The PCR product was subcloned into the pEGFP-C1 vector (Clontech, Mountain View, CA, USA). To generate double-stranded RNA for CD55, three parts of the DNA sequence, corresponding to nucleic acids 1–380, 381–817 and 821–1146 in the CD55 cDNA, were amplified by PCR. These sequences were named CD55-N, CD55-M and CD55-C, respectively. RNA transcription was then performed with this DNA template to generate sense and antisense single-stranded RNA. After production of double-stranded RNA, a reaction with the Dicer enzyme was carried out using a BLOCK-iT Dicer RNAi kit (Invitrogen). For siRNA for CD55, the siRNA was transfected into Raji and SK-BR3 cells using Lipofectamine 2000 (Invitrogen). In brief, 0.75 ng of siRNA and 5 μL of Lipofectamine 2000 in Optimen medium were mixed and incubated at room temperature for 20 min. The mixture was added to culture medium with SK-BR3 cells and fresh lymphoma cells, and the cells were incubated at 37°C for 72 h and 24 h, respectively. To see downregulation of CD55 expression, the CD55-transfected cells were stained with FITC-conjugated anti-CD55 antibody, and then expression of CD55 was observed without fixation of the cells at the same intensity of emission and excision as under laser scanning confocal fluorescent microscopy.

Statistical analysis

Correlation of susceptibility to CDC with tumor size, CD20 expression and CD55 expression were tested using the Spearman rank correlation coefficient. Statistical comparisons were carried out using two-sided Student's *t*-tests. All statistical analyses were performed using StatView 5.0 software (SAS Institute, Cary, NC, USA).

Results

Negative correlation between tumor size and susceptibility to CDC with rituximab

Rituximab is known to be effective at the early stages of indolent and aggressive lymphomas, but the effect of rituximab declines in some patients with bulky disease and a large number of lymphoma cells. According to this fact, we investigated whether susceptibility to CDC is dependent on the size of the tumor. The diameter of extirpated lymph nodes, CDC assay and CD20 expression were examined in fresh samples from 30 patients with lymphoma, as described in 'Materials and Methods'. As shown in Fig. 1a, the relationship between susceptibility to CDC and size of extirpated lymph nodes showed a significant negative correlation ($R = -0.895$, $P < 0.001$). In contrast, the relationship between susceptibility to CDC and CD20 expression, and between size of extirpated lymph nodes and CD20 expression, did not reveal significant correlations, as shown in Fig. 1b,c ($R = -0.076$, $P = 0.6807$ and 0.072, $P = 0.6979$, respectively). This suggests that susceptibility to CDC is dependent on the size of the lymphoma tumor, and that expression of CD20 does not contribute to susceptibility to CDC with rituximab in non-Hodgkin's lymphoma.

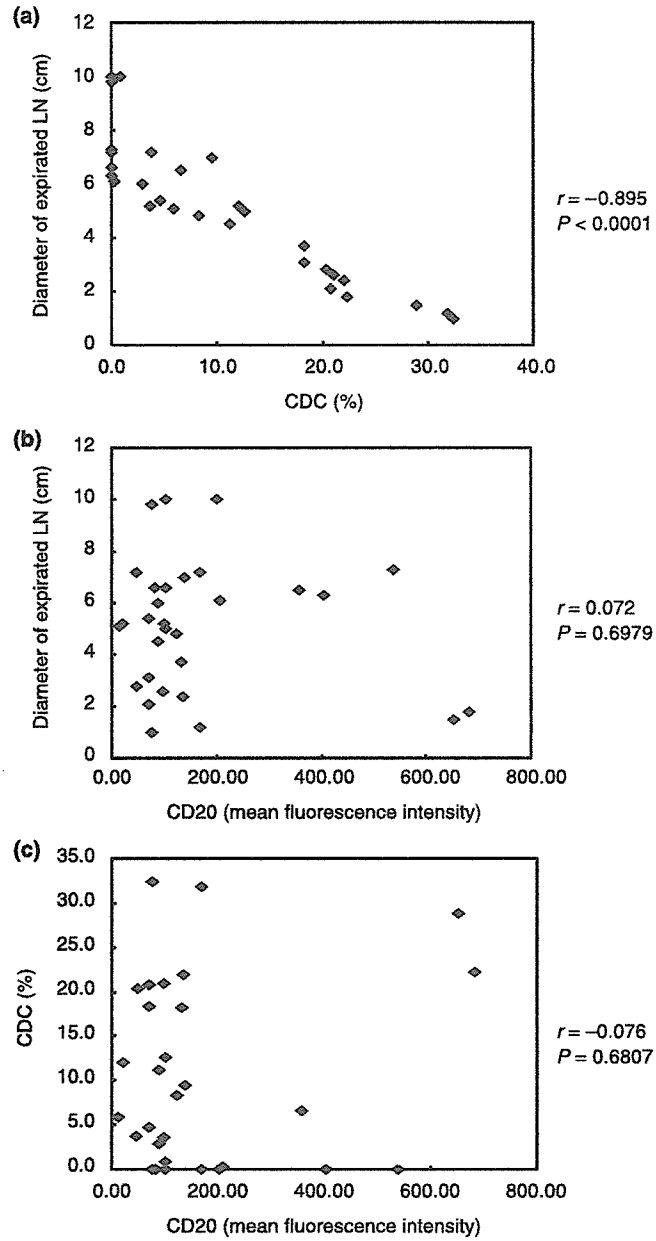

Fig. 1. Relationships between the size of extirpated tumors, susceptibility to complement-dependent cytotoxicity (CDC), and CD20 expression. The size of tumors from 30 patients with non-Hodgkin's lymphoma was measured and the cells were collected. After isolation of CD19-positive cells, FACScan analysis was carried out with anti-CD20 antibody, and CDC assay with rituximab was performed. Intensity of CD20 expression was normalized compared with a control. (a) Scatter plot and correlation analysis for size of extirpated tumor versus susceptibility to CDC. (b) Scatter plot and correlation analysis for size of extirpated tumor versus mean fluorescence intensity of CD20. (c) Scatter plot and correlation analysis for mean fluorescence intensity of CD20 versus susceptibility to CDC. All correlations were tested using the Spearman rank correlation coefficient.

doi: 10.1111/j.1349-7006.2006.00139.x

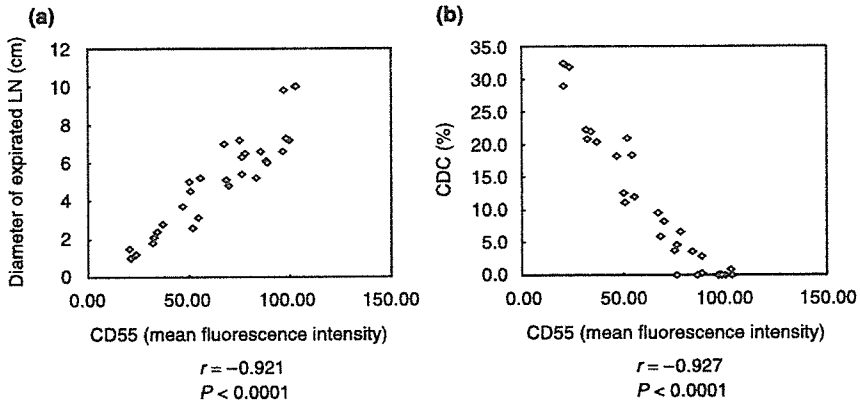

Fig. 2. Relationships between tumor size, CD55 expression and susceptibility to complement-dependent cytotoxicity (CDC). The size of tumors from 30 patients with lymphoma was measured and the cells were collected. After isolation of $CD19^+/CD20^+$ cells, FACscan analysis for CDC assay and CD55 expression were carried out. The intensity of CD55 expression was normalized compared with a control. (a) Scatter plot and correlation analysis for size of extirpated tumors versus CD55 expression. (b) Scatter plot and correlation analysis for CD55 expression versus susceptibility to CDC. All correlations were tested using the Spearman rank correlation coefficient.

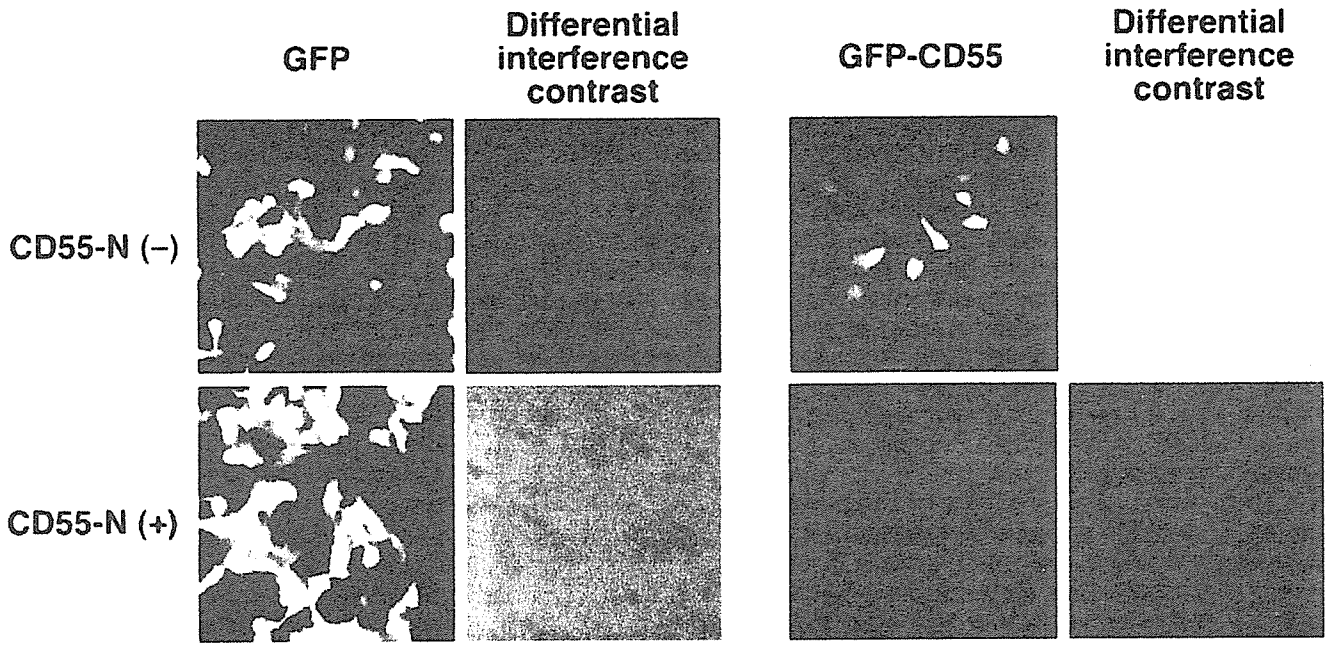

Fig. 3. Effect of small interfering RNA (siRNA) against the 5′-site of the *CD55* gene on expression of the exogenous *CD55* gene. MCF7 cells were transfected with pEGFP or pEGFP-CD55 in the presence or absence of siRNA. After 24 h, the cells were observed by laser scanning microscopy.

Size, CD55 expression and CDC in clinical samples

To investigate the relationship between the size of the extirpated tumor and CD55 expression in clinical samples, correlations between the size of extirpated tumor and fluorescence mean intensity of CD55, and between susceptibility to CDC with rituximab and fluorescence mean intensity of CD55, were analyzed statistically (Fig. 2). As shown in Fig. 2a, the level of CD55 expression on lymphoma cells was statistically correlated with the size of the lymph node ($r = 0.921$, $P < 0.001$). In contrast, the relationship between susceptibility to CDC with rituximab and fluorescence mean intensity of CD55 statistically revealed a negative correlation ($r = -0.927$, $P < 0.001$) (Fig. 2b). This suggests that increasing size of tumor contributes to higher or enhanced CD55 expression and resistance to CDC with rituximab.

Effect of siRNA for CD55 on CD55-transfected MCF7 cells

To overcome the resistance to CDC with rituximab on bulky mass, siRNA against a part of CD55 (CD55-N for 1–380 nucleotides) was designed and cotransfected with the pEGFP or pEGFP-CD55 plasmid into MCF7 cells (Fig. 3). When the cells were cotransfected with both pEGFP and siRNA for CD55, the expression of green fluorescent protein (GFP) did not change compared with transfection with only pEGFP vector (Fig. 3, upper panels). On the other hand, when the cells were cotransfected with both pEGFP-CD55 and siRNA for CD55, the expression of GFP-CD55 disappeared compared with transfection with only the pEGFP-CD55 vector (Fig. 3, lower panels). This suggests that CD55-N, siRNA against 1–380 nucleotides in the CD55 gene, is effective for blocking the expression of CD55.

Decrease in CD55 expression by siRNA overcomes resistance to CDC in breast cancer cell line SK-BR3

We investigated the use of a monoclonal antibody against the Her2/neu molecule for breast cancer, named trastuzumab.

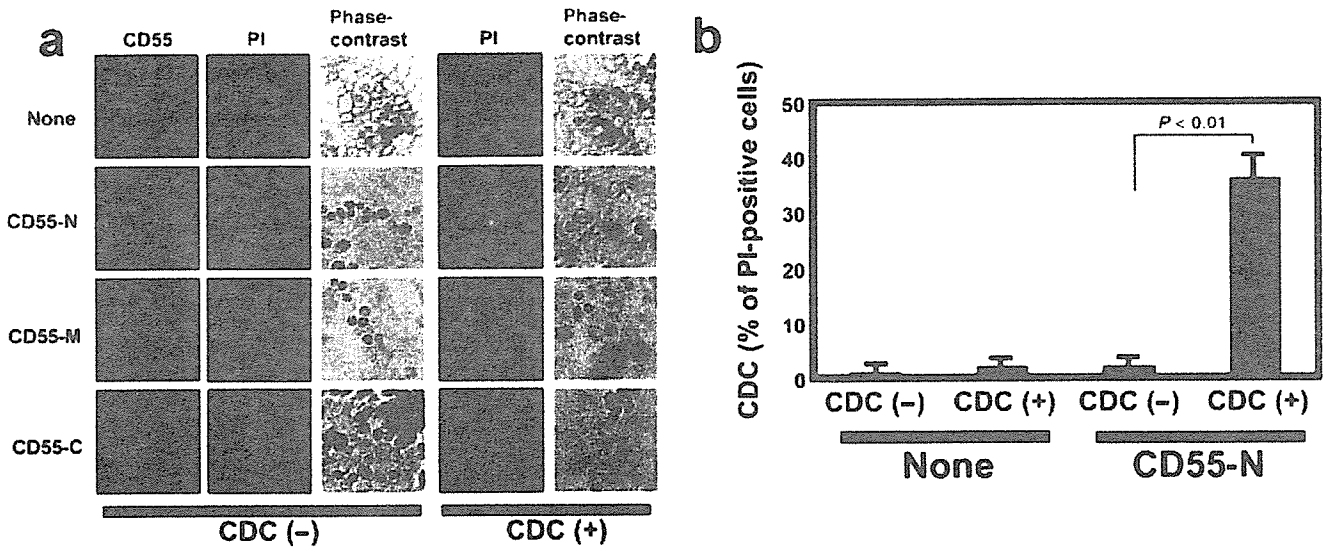

Fig. 4. Blockade of endogenous CD55 on breast cancer cells by small interfering RNA (siRNA). (a,b) SK-BR3 cells were transfected with siRNA against three parts of CD55, namely CD55-N, CD55-M and CD55-C, for 72 h. After transfection, the cells were stained with the anti-CD55 antibody and DAPI, and then the complement-dependent cytotoxicity (CDC) assay with trastuzumab was carried out with or without adding fresh human AB serum (a, left and right panels). (b) The percentage of propidium iodide-positive cells was calculated by counting 100 cells. Data are the mean ± SD (error bars) from experiments with triplicate samples. All statistical tests were two-sided Student's *t*-tests.

Because the breast cancer cell line SK-BR3 expresses Her2/neu and CD55 on its cell surface, siRNAs against three parts of CD55 (CD55-N for 1–380 nucleotides; CD55-M for 381–817 nucleotides; and CD55-C for 821–1146 nucleotides) were designed and introduced into SK-BR3 cells (Fig. 4). To detect dying cells, PI staining was used for the CDC assay with trastuzumab, and then the percentage of PI-positive cells was evaluated under laser scanning confocal microscopy. Most SK-BR3 cells expressed CD55 molecules without transfection of siRNA against CD55 (Fig. 4a, left). In contrast, expression of CD55 on SK-BR3 cells transfected with CD55-N disappeared 72 h after transfection, or became much weaker than without transfection of siRNA against CD55 (Fig. 4a, right). SK-BR3 cells transfected with CD55-M or CD55-C did not reveal knock down of CD55 expression to the level seen with CD55-N (Fig. 4a). Only 3.0 ± 1.0% of SK-BR3 cells without transfection of siRNA (mock transfection) against CD55 became PI-positive by CDC with trastuzumab, whereas 36.0 ± 6.0% of cells were PI-positive by CDC with trastuzumab after the transfection of siRNA (Fig. 4b). This suggested that siRNA against nucleotides 1–380 of CD55 (i.e. CD55-N) was effective for decreasing CD55 expression and sensitivity to CDC on adherent cells such as SK-BR3.

Blockade of CD55 expression by siRNA overcomes resistance to CDC in fresh lymphoma cells

To investigate the effect of siRNA against CD55 on fresh lymphoma cells, lymphoma cells were isolated from the lymph nodes of five patients with recurrent lymphomas and transfected with siRNA against CD55 (Fig. 5). As shown in Fig. 5a, lymphoma cells from all five cases with recurrent lymphoma strongly expressed CD55 molecules under laser scanning confocal microscopy. When fresh lymphoma cells were transfected with CD55-N for 24 h, but not CD55-M and CD55-C, CD55 expression on fresh lymphoma cells was significantly knocked down under laser scanning confocal microscopy, compared with the control (Fig. 5a, left columns). The percentage of PI-positive cells showed no significant differences among transfections with and without CD55-N, CD55-M and CD55-C before the CDC assay (Fig. 5b). The percentage of PI-positive cells in the transfection with CD55-N significantly increased from 7.1 ± 2.8% to 67.9 ± 8.1%. This indicates that the siRNA against CD55 (CD55-N) could efficiently knock down the expression of CD55 on SK-BR3 and freshly isolated lymphoma cells from recurrent lymphomas, and that it could induce cell death in SK-BR3 and freshly isolated lymphoma cells from recurrent lymphomas by CDC. This suggests that the degree of CD55 expression can determine resistance to CDC with antibody therapy, and that the therapies, which target CD55 molecules such as siRNA and its monoclonal antibody, would be helpful in antibody therapy for bulky disease.

Discussion

Treatment of malignancies has been largely based on chemotherapy and radiotherapy. Although improvement in response rates and survival has been obtained with these therapies over the years, a significant proportion of patients do not respond to treatment, or they relapse. Moreover, conventional cytotoxic therapy is often associated with significant morbidity. Recently, molecular targeting therapy has been developed[22] and monoclonal antibodies against CD20 and HER2/neu have been used for molecular targeting therapy.[1–3] Also, in recent therapies for malignancies, monoclonal antibodies have emerged as important therapeutic agents.

In the preset study, we have shown a negative correlation between the size of extirpated lymph nodes and susceptibility to CDC with rituximab, but the level of CD20 expression did

doi: 10.1111/j.1349-7006.2006.00139.x

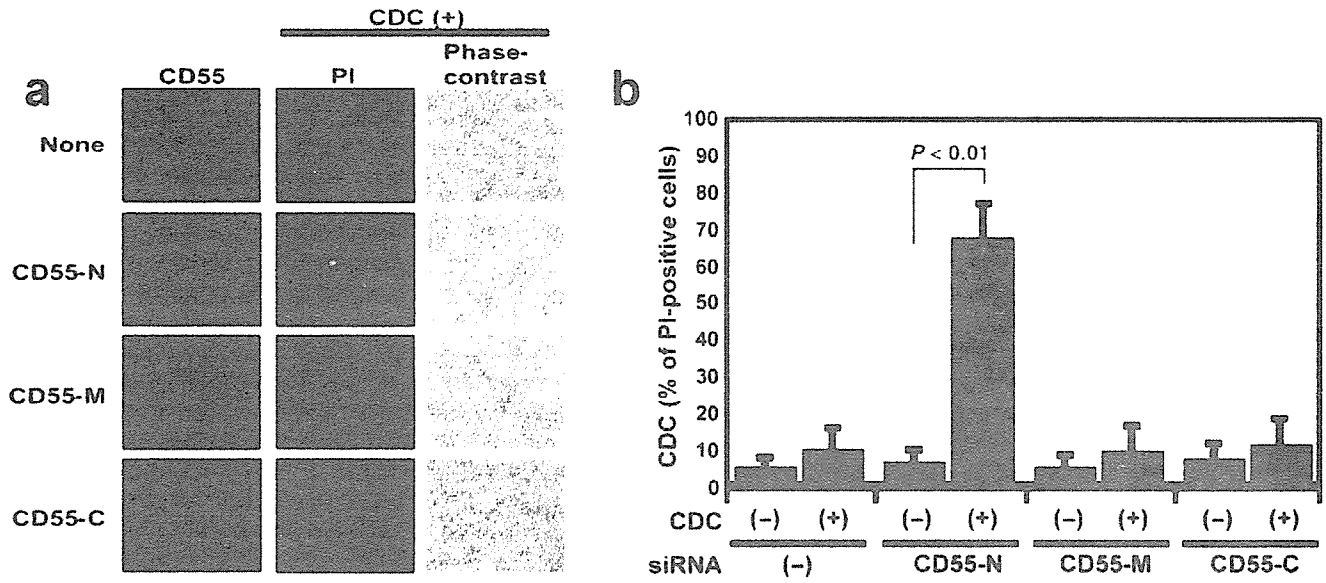

Fig. 5. Blockade of CD55 on primary lymphoma cells by small interfering RNA (siRNA). (a,b) Lymphoma cells from the lymph nodes of five patients with chemotherapy refractory and resistant lymphoma were transfected with siRNA against three parts of CD55, namely CD55-N, CD55-M and CD55-C, for 24 h. (a) After transfection, the cells were stained with anti-CD55 antibody and propidium iodide (PI), and then the complement-dependent cytotoxicity (CDC) assay with rituximab was carried out with or without adding fresh human AB serum. (b) The percentage of PI-positive cells was calculated by counting 100 cells. Data are the mean ± SD (error bars) from experiments with triplicate samples. All statistical tests were two-sided Student's *t*-tests.

not correlate with the size of the lymph node or susceptibility to CDC with rituximab. To date, no other studies have analyzed the relationship between size of lymph node and susceptibility to CDC with rituximab. It has been shown previously that CDC is directly correlated with CD20 expression.[11,23] In contrast, Manches *et al.*[24] have reported in detail that there is no direct correlation between lysis and expression of CD20 in global lymphoma such as FL, mantle cell lymphoma (MCL), small lymphocytic lymphoma (SLL), diffuse large B cell lymphoma (DLCL), and non-tumor B cells, as we showed in the current study. They also suggested that other regulators such as C-reactive protein (CRP) might play important roles in this complement system.

Although antibody therapy is a good tool, resistance sometimes occurs due to unknown mechanisms.[8,25] Patients with bulky mass, especially more than 7 cm of lymphoma mass, often show resistance to rituximab and are not curable.[26] We have demonstrated that CDC activity negatively correlates with the size of extirpated lymph nodes, and that the formula's intercept is 7.447 cm. This suggests that CDC is ineffective to tumors greater than 7.447 cm in size, and that our observation is consistent with the report of Coiffier *et al.*[26] Additionally, CD55 expression significantly correlates with the size of extirpated lymph nodes, suggesting that CD55 expression may play an important role in CDC resistance with antibody therapy. High densities of Daudi and Raji cells, associated with bulky mass, also became resistant to CDC with rituximab, and expression of CD55 increased during cell culture (Terui *et al.*, unpublished data). The relationship between cell density and size of tumors, resistance to CDC and CD55 expression are the same in not only extirpated lymph nodes from patients but also in experimental cell lines. Although previous reports have discussed whether CD55 can be an indicator of prognosis, no one has reported the relationship between cell density and tumor size, resistance to CDC and CD55 expression. Low or high CD55 expression has been reported in CLL cells.[11] However, some researchers have reported that *in vitro* susceptibility to rituximab-induced CDC could not be predicted by the levels of CD55 protein in CLL cells, nor *in vivo* in FL and CLL patients.[12,13] On the other hand, Golay *et al.*[27] have reported that relative levels of CD55 and CD59 may become useful markers to predict clinical responses. Overexpression of CD55 on some tumor cell lines and in colorectal carcinomas has been shown to be an indicator of poor prognosis. This result is consistent with the present study, as we found that CD55 expression in bulky disease may be a useful indicator of this prognosis. Recently, Madjd *et al.*[28] reported that loss of CD55 is related to poor prognosis in breast cancer. High expression of CD55 was significantly associated with low-grade lymph node negativity and with good prognosis. Survival analysis showed that CD55 overexpression was associated with a more favorable outcome. On the other hand, loss of CD55 is associated with poor survival. They established a novel anti-CD55 antibody for use in immunohistochemistry. Although they classified weak to strong intensity of CD55, it is possible that the antibody recognized the non-glycosylated SCR3 domain of CD55 molecule, but not the glycosylated CD55 molecule. The authors pointed out that loss of CD55 is associated with poor prognosis, but not with monoclonal antibody resistance. In the present study, we demonstrated that blockage of CD55 overcomes resistance to antibody therapy and that CDC plays an important role in tumor attack in antibody therapy. As the mechanism that we refer to is different from their study, it may depend on the type of cancer investigated.

Malignant progression has been reported to be associated with tumor hypoxia, and the inside of the bulky mass showed low oxygen partial pressure (PO_2) (<10 mmHg).[29] Because hypoxia induces COX-2 expression and prostaglandin E_2 (PGE_2) production in not only human vascular endothelial cells[30] but also tumor cells,[31,32] PGE_2 may be produced more in bulky tumors with hypoxia. Recently, it has been reported that PGE_2 upregulates expression of the complement inhibitor CD55 in colorectal cancer.[33] This suggests that bulky mass of lymphoma and other cancers may express CD55 to high levels via PGE_2 production.

It has been reported that the protective activity of rituximab or the 1F5 antibody is completely abolished in syngeneic knockout animals lacking C1q, the first component of the classical complement pathway C ($C1qa^{-/-}$).[34] This indicates that complement activation is fundamental for rituximab therapeutic activity *in vivo*. As CDC is more rapidly and efficiently triggered by monoclonal antibodies in cells with higher expression of their target molecules, we focused on how sensitivity to CDC can be recovered in the resistance to monoclonal antibody therapy. In antibody therapy, blockage of CD55 may be useful for recovery of sensitivity to CDC. It has been reported that anti-CD55 and anti-CD59 antibodies can enhance CDC sensitivity with rituximab, and that CD55 and CD59 may become useful markers to predict the clinical response.[24] Although they did not mention the therapy against resistance to antibody therapy using anti-CD55 and anti-CD59 antibodies,[24] there are three ways to block the function of CD55: (i) blocking the antibody against CD55; (ii) siRNA[35] for CD55; and (iii) small molecules as CD55 inhibitors. We have demonstrated that siRNA for CD55 successfully inhibited functional CD55 protein, and that CDC activity was enhanced in the CD55-knock down breast cancer cell line SK-BR3 and in clinical samples from lymphoma patients. In particular, siRNA is a better tool for blocking CD55, as siRNA can inhibit not only expression of CD55 but also the function of CD55. Nagajothi *et al.* also showed genetic and biochemical methods to decrease CD55 expression and other GPI-anchored proteins.[36] This suggests that a decline in CD55 levels could be enough to make the tumor sensitive to CDC with rituximab and trastuzumab.

In conclusion, we have shown that CD55 blockade by siRNA enhances rituximab-mediated cytotoxicity. This observation gives us a novel strategy to suppress bulky disease-related resistance to monoclonal antibody treatment.

Acknowledgments

This work was supported in part by a Grant-in-Aid from the Ministry of Education, Science and Culture of Japan; a Research on Advanced Medical Technology grant from the Ministry of Health, Welfare and Labor; and a grant for International Health Cooperation Research from the Ministry of Health, Welfare and Labor of Japan. We appreciate the assistance of Dr Dovie Wylie for English editing and correction, and thank Ms Tomomi Sagawa and Noriko Yamamichi for technical assistance.

References

1 Coiffier B. Immunochemotherapy: the new standard in aggressive non-Hodgkin's lymphoma in the elderly. *Semin Oncol* 2003; **30** (1 Suppl. 2): 21–7.
2 Tan AR, Swain SM. Ongoing adjuvant trials with trastuzumab in breast cancer. *Semin Oncol* 2003; **30** (5 Suppl. 16): 54–64.
3 Hiddemann W, Dreyling M, Unterhalt M. Rituximab plus chemotherapy in follicular and mantle cell lymphomas. *Semin Oncol* 2003; **30** (1 Suppl. 2): 16–20.
4 Dillman RO. Treatment of low-grade B-cell lymphoma with the monoclonal antibody rituximab. *Semin Oncol* 2003; **30**: 434–47.
5 Blum KA, Bartlett NL. Antibodies for the treatment of diffuse large cell lymphoma. *Semin Oncol* 2003; **30**: 448–56.
6 Grillo-Lopez AJ. Rituximab: an insider's historical perspective. *Semin Oncol* 2000; **27** (6 Suppl. 12): 9–16.
7 Maloney DG, Smith B, Rose A. Rituximab: mechanism of action and resistance. *Semin Oncol* 2002; **29** (1 Suppl. 2): 2–9.
8 Villamor N, Montserrat E, Colomer D. Mechanism of action and resistance to monoclonal antibody therapy. *Semin Oncol* 2003; **30**: 424–33.
9 Wojnicz D, Bar J, Jankowski S. [The role of membrane glycoproteins CD46, CD55 and CD59 in protection of tumor cells against complement lysis]. *Postepy Hig Med Dosw* 2002; **56** (5): 603–16. (In Polish.)
10 Cerny T, Borisch B, Introna M, Johnson P, Rose AL. Mechanism of action of rituximab. *Anticancer Drugs* 2002; 13 (Suppl. 2): S3–10.
11 Bellosillo B, Villamor N, Lopez-Guillermo A *et al.* Complement-mediated cell death induced by rituximab in B-cell lymphoproliferative disorders is mediated *in vitro* by a caspase-independent mechanism involving the generation of reactive oxygen species. *Blood* 2001; **98**: 2771–7.
12 Bannerji R, Kitada S, Flinn IW *et al.* Apoptotic-regulatory and complement-protecting protein expression in chronic lymphocytic leukemia: relationship to *in vivo* rituximab resistance. *J Clin Oncol* 2003; **21**: 1466–71.
13 Weng WK, Levy R. Expression of complement inhibitors CD46, CD55, and CD59 on tumor cells does not predict clinical outcome after rituximab treatment in follicular non-Hodgkin lymphoma. *Blood* 2001; **98**: 1352–7.
14 Cardarelli PM, Quinn M, Buckman D *et al.* Binding to CD20 by anti-B1 antibody or F (ab') (2) is sufficient for induction of apoptosis in B-cell lines. *Cancer Immunol Immunother* 2002; **51**: 15–24.
15 Hourcade D, Liszewski MK, Krych-Goldberg M, Atkinson JP. Functional domains, structural variations and pathogen interactions of MCP, DAF and CR1. *Immunopharmacology* 2000; **49**: 103–16.
16 Jarva H, Meri S. Paroxysmal nocturnal haemoglobinuria: the disease and a hypothesis for a new treatment. *Scand J Immunol* 1999; **49**: 119–25.
17 Jeremias I, Kupatt C, Baumann B, Herr I, Wirth T, Debatin KM. Inhibition of nuclear factor κB activation attenuates apoptosis resistance in lymphoid cells. *Blood* 1998; **9**: 4624–31.
18 Unruh A, Ressel A, Mohamed HG *et al.* The hypoxia-inducible factor-1α is a negative factor for tumor therapy. *Oncogene* 2003; **22**: 3213–20.
19 Elbashir SM, Harborth J, Lendeckel W, Yalcin A, Weber K, Tuschl T. Duplexes of 21-nucleotide RNAs mediate RNA interference in cultured mammalian cells. *Nature* 2001; **411**: 494–8.
20 Pham LV, Tamayo AT, Yoshimura LC, Lin-Lee YC, Ford RJ. Constitutive NF-κB and NFAT activation in aggressive B cell lymphomas synergistically activates the CD154 gene and maintains lymphoma cell survival. *Blood* 2005; **106**: 3940–7.
21 Surmacz E. Growth factor receptors as therapeutic targets: strategies to inhibit the insulin-like growth factor I receptor. *Oncogene* 2003; **22**: 6589–97.
22 Gale DM. Molecular targets in cancer therapy. *Semin Oncol Nurs* 2003; **19**: 193–205.
23 Golay J, Lazzari M, Facchinetti V *et al.* CD20 levels determine the *in vitro* susceptibility to rituximab and complement of B-cell chronic lymphocytic leukemia: further regulation by CD55 and CD59. *Blood* 2001; **98**: 3383–9.
24 Manches O, Lui G, Chaperot L *et al.* *In vitro* mechanisms of action of rituximab on primary non-Hodgkin lymphomas. *Blood* 2003; **101**: 949–54.
25 Smith MR. Rituximab (monoclonal anti-CD20 antibody): mechanisms of action and resistance. *Oncogene* 2003; **22**: 7359–68.
26 Coiffier B, Haioun C, Ketterer N *et al.* Rituximab (anti-CD20 monoclonal antibody) for the treatment of patients with relapsing or

doi: 10.1111/j.1349-7006.2006.00139.x

refractory aggressive lymphoma: a multicenter phase II study. *Blood* 1998; **92**: 1927–32.
27 Golay J, Zaffaroni L, Vaccari T *et al.* Biologic response of B lymphoma cells to anti-CD20 monoclonal antibody rituximab *in vitro*: CD55 and CD59 regulate complement-mediated cell lysis. *Blood* 2000; **95**: 3900–8.
28 Madjd Z, Durrant LG, Bradley R, Spendlove I, Ellis IO, Pinder SE. Loss of CD55 is associated with aggressive breast tumors. *Clin Cancer Res* 2004; **10**: 2797–803.
29 Hockel M, Schlenger K, Aral B, Mitze M, Schaffer U, Vaupel P. Association between tumor hypoxia and malignant progression in advanced cancer of the uterine cervix. *Cancer Res* 1996; **56**: 4509–15.
30 Schmedtje JF Jr, Ji YS, Liu WL, DuBois RN, Runge MS. Hypoxia induces cyclooxygenase-2 via the NF-κB p65 transcription factor in human vascular endothelial cells. *J Biol Chem* 1997; **272**: 601–8.
31 Liu XH, Kirschenbaum A, Yu K, Yao S, Levine AC. Cyclooxygenase-2 suppresses hypoxia-induced apoptosis via a combination of direct and indirect inhibition of p53 activity in a human prostate cancer cell line. *J Biol Chem* 2005; **280**: 3817–23.
32 Liu XH, Kirschenbaum A, Yao S *et al.* Upregulation of vascular endothelial growth factor by cobalt chloride-simulated hypoxia is mediated by persistent induction of cyclooxygenase-2 in a metastatic human prostate cancer cell line. *Clin Exp Metastasis* 1999; **17**: 687–94.
33 Holla VR, Wang D, Brown JR, Mann JR, Katkuri S, DuBois RN. Prostaglandin E2 regulates the complement inhibitor CD55/decay-accelerating factor in colorectal cancer. *J Biol Chem* 2005; **280**: 476–83.
34 Di Gaetano N, Cittera E, Nota R *et al.* Complement activation determines the therapeutic activity of rituximab *in vivo*. *J Immunol* 2003; **171**: 1581–7.
35 Elbashir SM, Harborth J, Lendecke W, Yalcin A, Weber K, Tuschl T. Duplexes of 21-nucleotide RNAs mediate RNA interference in cultured mammalian cells. *Nature* 2001; **411**: 494–8.
36 Nagajothi N, Matsui WH, Mukhina GL, Brodsky RA. Enhanced cytotoxicity of rituximab following genetic and biochemical disruption of glycosylphosphatidylinositol anchored proteins. *Leuk Lymphoma* 2004; **45**: 795–9.

J. Biochem. **139**, 761–769 (2006)
doi:10.1093/jb/mvj079

Amino Acids C-Terminal to the 14-3-3 Binding Motif in CDC25B Affect the Efficiency of 14-3-3 Binding

Sanae Uchida[1], Akitsugu Kubo[1], Ryoichi Kizu[2,*], Hitoshi Nakagama[3], Tsukasa Matsunaga[1], Yukihito Ishizaka[4] and Katsumi Yamashita[1,5]

[1]Division of Life Science and [2]Division of Environmental Science and Engineering, Graduate School of Science and Technology, Kanazawa University, Kakuma-machi, Kanazawa, Ishikawa 920-1192; [3]Biochemistry Division, National Cancer Center Research Institute, 1-1 Tsukiji 5-chome, Chuo-ku, Tokyo 104-0045; [4]Division of Intractable Disease, International Medical Center of Japan, 21-1 Toyama 1-chome, Shinjyuku-ku, Tokyo 162-8655; and [5]Cancer Research Institute, Kanazawa University, 13-1 Takara-machi, Kanazawa, Ishikawa 920-0934

Received February 8, 2006; accepted February 21, 2006

The phospho-site adapter protein 14-3-3 binds to target proteins at amino acid sequences matching the consensus motif Arg-X-X-Ser/Thr-X-Pro, where the serine or threonine residue is phosphorylated and X is any amino acid. The dual-specificity phosphatase CDC25B, which is involved in cell cycle regulation, contains five 14-3-3 binding motifs, but 14-3-3 preferentially binds to the motif at Ser309 in CDC25B1 (or Ser323 in CDC25B3). In the present study, we demonstrate that amino acid residues C-terminal to the 14-3-3 binding motif strongly affect the efficiency of 14-3-3 binding. Alanine substitutions at residues downstream of the Ser309 motif dramatically reduced 14-3-3 binding, although phosphorylation of Ser309 was unaffected. We also observed that binding of endogenous 14-3-3 to mutant CDC25B occurred less efficiently than to the wild type. Mutants to which 14-3-3 cannot bind efficiently tend to be located in the nucleus, although not as specifically as the alanine substitution mutant of Ser309. These results indicate that amino acid sequences C-terminal to the consensus binding site have an important role in the efficient binding of 14-3-3 to at least CDC25B, which may partly explain why some consensus sequences are inactive as 14-3-3 binding sites.

Key words: 14-3-3, CDC25B, cell cycle, phosphorylation, subcellular localization.

Abbreviations: CDK, cyclin-dependent kinase; GST, glutathione-S-transferase; MAPKAP, mitogen-activated protein kinase–activated protein; MK2, MAPKAP kinase 2; NLS, nuclear localization signal.

The eukaryotic cell cycle progresses through successive cycles of activation and inactivation of cyclin-dependent kinases (CDKs) that are complexed with cyclins. The activities of these complexes are regulated via several mechanisms, including inhibition of CDK by small proteins (*e.g.*, p16, p21, and p27), inhibitory phosphorylation by Wee1/Myt1 kinases at the ATP binding site of CDK, and activation of dephosphorylation by CDC25 dual-specificity phosphatases.

Three CDC25 phosphatases have been identified in mammalian cells, CDC25A, CDC25B, and CDC25C (*1*). The first CDC25 phosphatase gene to be identified was that encoding CDC25C, which dephosphorylates phospho-Tyr15 of CDK1 (previously phosphorylated by Wee1 kinase) to promote the G2 to M phase transition (*2*, *3*). Studies using cultured mammalian cells have suggested that CDC25A plays a role in the G1 to S phase transition by activating CDK2/cyclin E (*4*, *5*), and that CDC25B and CDC25C function in M phase entry by activating and maintaining CDK1:cyclin B activity during the M phase (*6–9*).

*To whom correspondence should be addressed at the present address: Department of Environmental Biochemistry, Faculty of Pharmaceutical Sciences, Doshisha Women's College of Liberal Arts, Kodo, Kyotanabe 610-0395. Tel: +81 76 264 5809, Fax: +81 76 264 5989, E-mail: katsumi@kenroku.kanazawa-u.ac.jp

Recent reports provided evidence that CDC25A also plays an important role in the G2 to M phase transition, thus indicating that CDC25A regulates all cell cycle stages (*10*, *11*). However, mice depleted of CDC25C by gene targeting develop normally and become fertile adults (*12*), and CDC25B knockout mice are born essentially healthy, although the females are sterile because of a defect in oogenesis (*13*). A recent report confirmed that mice lacking both the CDC25B and CDC25C genes are born healthy and that cells derived from these mice not only undergo normal entry to the M phase but also exhibit no checkpoint defects (*14*). Therefore, CDC25B and CDC25C are not essential for mouse development and for DNA damage checkpoints.

CDC25 proteins are CDK activators and, as a result, may comprise important cell cycle checkpoints (*15–17*). When the cell cycle checkpoint kinase CHK1 or CHK2 is activated by genotoxic stress, it phosphorylates several serine or threonine residues in CDC25A, which leads to the ubiquitin-proteasome pathway-mediated degradation of CDC25A that accompanies cell cycle arrest at the G1, G2, or intra-S phase (*10*, *17*). CDC25B and CDC25C, as well as CDC25A, are good substrates for CHK1 and CHK2 *in vitro* (*18–20*). CDC25B overexpression overrides the G2 checkpoint after ionizing radiation and other genotoxic stresses, and overproduction of a non-phosphorylated

mutant form of CDC25C partially overrides the G2 checkpoint (*21–24*).

One of the phospho-site adapter proteins, 14-3-3, appears to be centrally involved in the CDC25 function, especially in terms of checkpoint function (*15*, *22–25*). CHK1 and CHK2 [and very recently mitogen-activated protein kinase-activated protein (MAPKAP) kinase 2 (MK2)] have been shown to phosphorylate CDC25B and CDC25C at phosphorylation sites containing the 14-3-3 consensus binding sequence (*23*, *24*, *26*). The binding of 14-3-3 to CDC25B or CDC25C may recruit these phosphatases to the cytoplasm from the nucleus and help to retain them there, thus preventing CDK1 activation in the nucleus (*27–30*). However, CDC25 phosphorylation by CHK1 or CHK2 down-regulates its phosphatase activity, in both 14-3-3 binding–dependent and –independent manners (*31–33*). At this point, the precise role of CDC25 binding to 14-3-3 in the normal cell cycle and its checkpoints remains to be defined.

We previously reported that 14-3-3β and 14-3-3ε can bind to Ser309 phosphorylation site in CDC25B1, and that the single phosphorylation at Ser309 is sufficient to sustain the binding of the β and ε 14-3-3 isoforms (*30*). In the present study, we further examined the importance of 14-3-3 binding in the regulation of CDC25B. We studied binding to CDC25B of other 14-3-3 isoforms, such as 14-3-3γ, η, θ, which is also called τ, and ζ and found that they bind primarily to the Ser309 site. Furthermore, our results reveal major roles not only for the amino acids in the Ser309 consensus site but also for the amino acids surrounding the consensus site in efficient 14-3-3 binding.

EXPERIMENTAL PROCEDURES

Cell Culture and Transformation—HEK293, Cos-7, and HeLa cells (American Type Culture Collection strains CRL-1573, CRL-1651, and CCL-2, respectively) were grown in Dulbecco's Modified Eagle's Medium supplemented with 10% fetal bovine serum, 100 μg/ml penicillin, 100 U/ml streptomycin, and 50 μg/ml M-Plasmocin under a humidified atmosphere of 5% CO_2. Fetal bovine serum, penicillin, and streptomycin were from Sigma (St. Louis, MO, USA), and M-Plasmocin from Invivogen (San Diego, CA, USA). For the transformation of HEK-293 and Cos-7 cells, appropriate amounts of DNA were transfected with FuGENE6 (Roche Diagnostics, Indianapolis, IN, USA). HeLa cells were transfected with LipofectAMINE2000 (Invitrogen, Carlsbad, CA, USA) according to the manufacturer's recommendation.

Plasmid Construction—Plasmids encoding N-terminal double FLAG-tagged CDC25B1, and N-terminal double myc-tagged 14-3-3β, ε, and σ were constructed as described previously (*30*). For the isolation of the other 14-3-3 subtypes, the coding regions were amplified by PCR using specific primers for 14-3-3γ, η, θ, and ζ. Each amplified fragment was subcloned into a modified pEF6-mycHisB vector (Invitrogen) such that a double Myc-tag was encoded at each N-terminus. The sequences of these primers are shown in Table 1. Human CHK1 and CHK2 were provided by Steve Elledge of Harvard Medical School. Human MK2 cDNA was purchased from Open Biosystems (Huntsville, AL, USA). All were amplified with specific primers (Table 1) and subcloned into modified pEF6-mycHisB such that a double HA tag was encoded at the N- or C-terminus and a 6×His tag was encoded at the C-terminus. The GST-CDC25B peptide expression plasmid was constructed by PCR amplification of the CDC25B gene, digestion of the PCR product with *Nco*I and *Xho*I, and ligation into the pGEX-KG vector (*34*). The primers used to amplify CDC25B are shown in Table 1.

Site-Directed Mutagenesis—PCR-based site-directed mutagenesis with complementary oligonucleotide pairs was used to insert alanine point mutations in CDC25B, and to place a *Bam*HI restriction site between Leu319 and Lys320 of CDC25B. The sequence of one strand of each primer pair is shown in Table 2.

Antibodies—Antisera against a phospho-Ser309 peptide (*23*) and the FLAG tag (*35*) were raised as described and affinity purified. Anti-myc and anti-HA antibodies were from Cell Signaling (Beverly, MA, USA), anti-GST

Table 1. **PCR primers used for amplification and construction of tagged proteins.**

Gene	Primer	DNA sequence (5′→3′)
14-3-3γ	Forward	AGCCCCGGATCCATGGTGGACCGCGAGCAACTGGTG
	Reverse	TCCCCTGAATTCTTAATTGTTGCCTTCGCCGCCATC
14-3-3η	Forward	CCGAGCCGGATCCCATATGGGGGACCGGGAGCAGCTGCTG
	Reverse	CCTGAAGAATTCTCAGTTGCCTTCTCCTGCTTCTTC
14-3-3θ	Forward	CCCGCGGGATCCATGGAGAAGACTGAGCTGATCCAG
	Reverse	ACACCCGAATTCGATTTAGTTTTCAGCCCCTTCTGC
14-3-3ζ	Forward	GAACATGGATCCATGGATAAAAAATGAGCTGGTTCAG
	Reverse	AAGTTGGAATTCCGGTTAATTTTCCCCTCCTTCTTC
CHK1	Forward	CTCGGTCTAGACATGGCAGTGCCCTTTGTG
	Reverse	GCCGATGGTGATATCATGTGGCAGGAAGCC
CHK2	Forward	GCTCACGGTACCGCCATGTCTCGGGAGTCG
	Reverse	TTCAAACCACGGGATATCCAACACAGCAGC
MK2	Forward	TCCCCGGGTACCATGCTGTCCAACTCCCAGGGCCAG
	Reverse	CGCGGTGATATCGTGGGCCAGAGCCGCAGCCTCCAGGG
MKK6	Forward	AAGGGGCATATGTCTCAGTCGAAAGGCAAGAAGCGAAACCCTGGC
	Reverse	GTCCACGATATCTTAGTCTCCAAGAATCAGTTTTACAAAAGATGC
GST-CDC25B	Forward	GTTCCCCCAGCCATGGAGAGTCTCATTAGT
	Reverse	TGATTTTGACTCGAGCTAGCGGGCTTTAGG

Table 2. **Sequences of primer pairs used for PCR-based site-directed mutagenesis of CDC25B.**

Mutation	Forward primer sequence (5′→3′)
Leu304Ala	AAGTGCCAGCGGGCCTTCCGCTCTCCG
Arg306Ala	CAGCGGCTCTTCGCCTCTCCGTCCATG
Ser309Ala	CTCTTCCGCTCTCCGGCCATGCCCTGCAGC
Met310Ala	CGCTCTCCGTCCGCCCCCTGCAGCGTG
Pro311Ala	TCTCCGTCCATGGCCTGCAGCGTGATC
Cys312Ala	CCGTCCATGCCCGCCAGCGTGATCCGG
Ser313Ala	TCCATGCCCTGCGCCGTGATCCGGCCC
Val314Ala	ATGCCCTGCAGCGCCATCCGGCCCATC
Ile315Ala	CCCTGCAGCGTGGCCCGGCCCATCCTC
Arg316Ala	TGCAGCGTGATCGCTCCCATCCTCAAG
Pro317Ala	AGCGTGATCCGGGCCATCCTCAAGAGG
Ile318Ala	GTGATCCGGCCCGCCCTCAAGAGGCTG
Leu319Ala	ATCCGGCCCATCGCCAAGAGGCTGGAG
319/BamHI/320	CGGCCCATCCTCGGATCCAAGAGGCTGGAG

serum from Amersham Biosciences (Piscataway, NJ, USA), and anti-FLAG M2-beads from Sigma.

Preparation of Cell Extracts, Immunoprecipitation, and Immunoblotting—Crude cell extracts were prepared as described previously (*30*). Cells were collected by scraping, washed in ice-cold phosphate-buffered saline (PBS), and lysed with immunoprecipitation (IP) buffer (50 mM Tris-HCl, pH 7.5, 150 mM NaCl, 0.5% NP-40, 5 mM EGTA, and 1 mM EDTA) supplemented with protease and phosphatase inhibitor mixes as described previously (*30*). Cell extracts were centrifuged at 15,000 × *g* for 10 min at 4°C, the supernatant fractions were collected, and the protein concentrations were determined by the Bradford method (Bio-Rad, Richmond, CA, USA) (*36*). For immunoprecipitation, typically 500 μg of protein was mixed with anti-FLAG M2-agarose beads or 2 μg of anti-myc monoclonal antibodies followed by protein G-Sepharose beads (Amersham Biosciences). Crude cell extracts or immunoprecipitates were subjected to immunoblotting using rabbit polyclonal anti-FLAG antibodies (for CDC25B), mouse monoclonal anti-myc antibodies (for 14-3-3), or mouse monoclonal anti-HA antibodies (for kinases).

Protein Purification—Protein kinases were prepared from cDNA-transfected Cos-7 cells. Typically, 8 × 10^5 Cos-7 cells in a 6-cm dish received 4 μg of plasmid DNA with FuGENE6. After 24 h, the cells were collected, washed with PBS, and lysed with EDTA-free IP buffer supplemented with a 1:100 dilution of FOCUS Protease Arrest (EMD Biosciences, San Diego, CA, USA), 20 mM *p*-nitrophenyl phosphate, 20 mM NaF, and 20 mM β-glycerophosphate. To purify the kinases, Ni^{2+}-charged immobilized metal-chelating Sepharose beads (Amersham Biosciences) were added to the cell extracts containing 1.5 mg protein, and the protein-bound beads were used directly in kinase assays. GST-tagged proteins were expressed in *Escherichia coli* BL21 (DE3) cells transformed with the appropriate cDNA plasmid constructs. Expression was induced with 0.4 mM isopropyl-β-D-thiogalactopyranoside, and proteins were purified with glutathione–Sepharose beads (Amersham Biosciences).

Indirect Immunofluorescence Microscopy—Indirect immunofluorescence analysis was performed as described previously (*30*, *37*). Transfected HEK293 cells were fixed with 3.7% formaldehyde and then permeabilized with 0.5% Triton X-100. Expressed CDC25B proteins were detected with rabbit polyclonal anti-FLAG antibodies, followed by AlexaFluor 594– or 488–conjugated goat anti-rabbit IgG (Molecular Probes, Eugene, OR, USA), and expressed 14-3-3 was detected with mouse monoclonal anti-Myc antibodies and AlexaFluor 488–conjugated goat anti-mouse IgG. Nuclei were stained with 4′,6-diamino-2-phenylindole (Sigma).

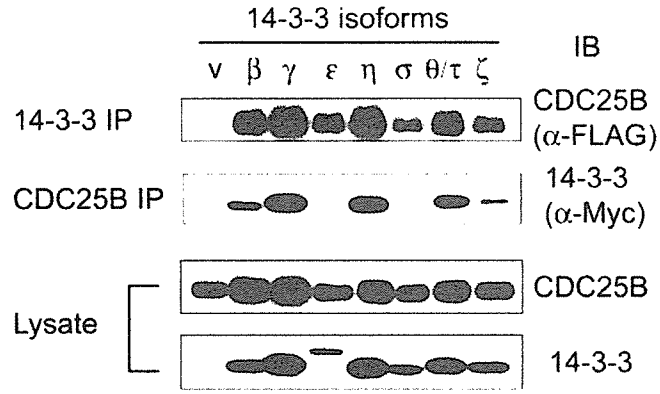

Fig. 1. **Binding of 14-3-3 subtypes to CDC25B.** HEK293 cells (1.4 × 10^6 cells per 35-mm plate) were transfected with 3 μg of FLAG-tagged CDC25B DNA and 0.6 μg of myc-tagged 14-3-3 DNA. The cells were collected 24 h after transfection, and cell extracts were prepared. The cell extracts were either subjected to Western blotting to visualize protein expression or further processed for immunoprecipitation with anti-FLAG or anti-myc antibodies to analyze binding. Upper panel: IP with anti-myc (14-3-3), followed by IB with anti-FLAG (CDC25B); second panel: IP with anti-FLAG (CDC25B), followed by IB with anti-myc (14-3-3).

RESULTS

All Seven Isoforms of 14-3-3 Bind to CDC25B—We previously showed that 14-3-3 isoforms β, ε, and σ bind efficiently to CDC25B, with the β and ε isoforms binding preferentially to the 14-3-3 binding motif at Ser309 (309 site), and the σ isoform binding preferentially to the motif at Ser216 (216 site) (*30*). In the present study, we analyzed the binding properties of four additional isoforms of 14-3-3. The genes for the γ, η, θ, and ζ isoforms were amplified by PCR and expressed in HEK293 cells. Each 14-3-3 isoform was co-expressed with CDC25B, isolated, and analyzed as to its interaction with CDC25B. As shown in Fig. 1, all the14-3-3 isoforms were able to interact with CDC25B. CDC25B was detected in immunoprecipitates of all the 14-3-3 isoforms (Fig. 1, upper panel), and all the 14-3-3 isoforms were recovered in the CDC25B co-immunoprecipitates (Fig. 1, second panel). Taking the protein expression levels into account, the 14-3-3ε, σ, and ζ isoforms appeared to bind more weakly to CDC25B than did the other 14-3-3 isoforms (Fig. 1, second and fourth panels).

As we reported previously (*30*), CDC25B has five 14-3-3 consensus binding motifs (Fig. 2A). Here, we examined the CDC25B binding site preference of each 14-3-3 isoform using co-transfection with plasmids encoding various CDC25B mutants. Five of these mutants contained

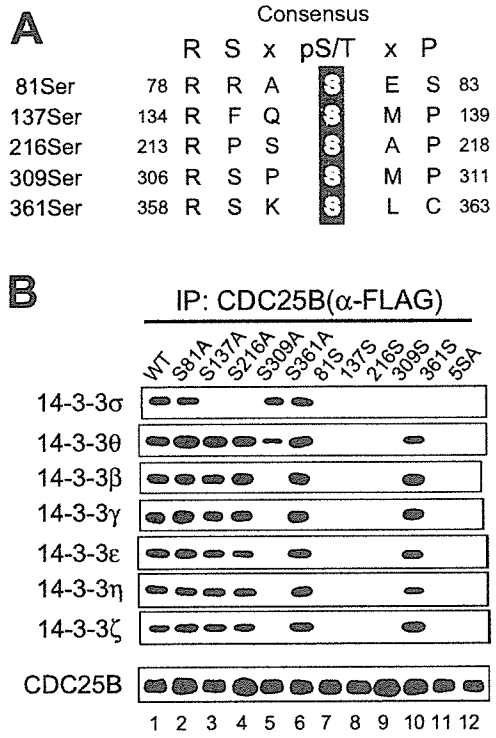

C

14-3-3 subtype	CDC25B mutants											
	WT	S81A	S137A	S216A	S309A	S361A	81S	137S	216S	309S	361S	5SA
σ	++	++	+	–	++	++	–	–	±	–	–	–
θ	++	++	++	++	+	++	–	–	–	++	–	–
β	++	++	++	++	–	++	–	–	–	++	–	–
γ	++	++	++	++	±	++	–	–	–	++	–	–
ε	++	++	++	++	±	++	–	–	–	++	–	–
η	++	++	++	++	–	++	–	–	–	++	–	–
ζ	++	++	++	++	±	++	–	–	–	++	–	–

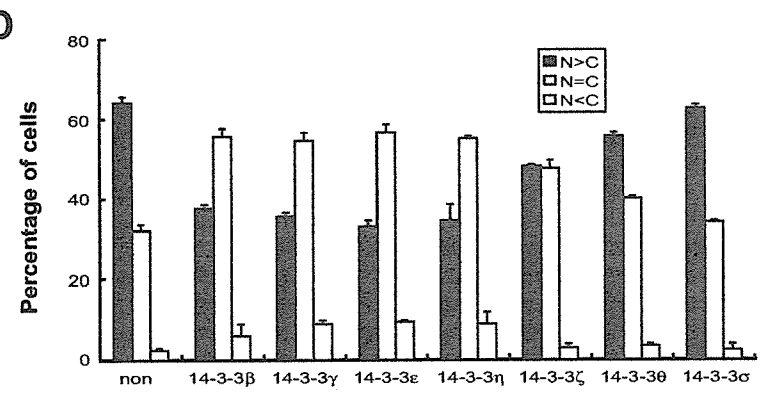

Fig. 2. **CDC25B binding site preferences of 14-3-3 subtypes.** FLAG-tagged CDC25B mutants with Ser→Ala substitutions at possible 14-3-3 binding sites (*30*) were co-transfected with each 14-3-3 subtype, as described in Fig. 1. Cell extracts were prepared 24 h after transfection and then immunoprecipitated with anti-FLAG-agarose beads to recover the CDC25B mutant proteins. Recovered CDC25B and co-immunoprecipitated 14-3-3 were detected by Western blotting. A: Possible 14-3-3 consensus binding sites and their amino acid sequences. B: Isoforms of 14-3-3 recovered with anti-FLAG-agarose beads. The bottom panel indicates a typical result of expression of co-transfected CDC25B mutants. C. Summary of the results shown in B. ++, strong signal; +, moderate signal; ±, discernible after long exposure; –, no signal. D. Subcellular localization of wild-type CDC25B upon co-expression with 14-3-3 subtypes. Cover slips in 35-mm plates were seeded with 2×10^5 HEK293 cells. After 2 days, the cells were transfected with myc-tagged 14-3-3 subtypes in combination with FLAG-tagged wild-type CDC25B. The cells were fixed 24 h after transfection, and the subcellular localization of CDC25B was determined by staining with anti-FLAG antibodies. More than 200 cells were examined. The data shown are the averages of three independent experiments. Bars = standard deviation.

single-site Ser→Ala substitutions in one 14-3-3 binding motif (*e.g.*, mutant Ser309Ala). In addition, the 309Ser mutant contained Ser→Ala substitutions at all possible binding sites except site 309, and the 5SerAla mutant contained Ser→Ala substitutions at all five putative binding sites.

CDC25B immunoprecipitates were recovered from cells co-transfected with the *14-3-3* and mutant *CDC25* genes, and 14-3-3 was detected on Western blots. All 14-3-3 isoforms except 14-3-3σ were found to bind preferentially to site 309 (Fig. 2B), as shown previously (*30*). Although substantial binding of 14-3-3θ to the Ser309Ala mutant did occur, comparison with the other single-site mutations revealed that 14-3-3θ bound preferentially to site 309. These results are summarized in Fig. 2C.

We examined the effect of co-transfection with 14-3-3 isoforms on the subcellular localization of CDC25B. Previously, we found that the binding of 14-3-3 at site 309 caused CDC25B to move from the nucleus to the cytoplasm (*30*). In the present study, we found that 14-3-3 isoforms that preferentially bound at site 309 caused CDC25B to be exported from the nucleus to the cytoplasm, and that isoforms that bound weakly or non-preferentially to site 309 did not have such an effect (Fig. 2D). The 14-3-3θ isoform, which binds preferentially to site 309, exhibited a mobilizing effect on the 309Ser mutant (data not shown), consistent with the results of the binding analysis above.

Mutations Near Ser309 of CDC25B Interfere with 14-3-3 binding—The effects of co-transfection with 14-3-3 on the cytoplasmic distribution of CDC25B indicated that 14-3-3 binding at site 309 may have masked the nuclear localization signal (NLS) sequence of CDC25B, which begins about ten residues downstream of the binding site (Fig. 3A). We therefore conducted experiments to determine the effect of an increased distance between Ser309 and the NLS sequence. Lys320 is the first residue of the bipartite NLS sequence in CDC25B. To enable the in-frame insertion of additional amino acids, we initially used mutagenesis to introduce a *Bam*HI site between residues 319 and 320. The *Bam*HI recognition sequence resulted in the insertion of Gly–Ser (GS) dipeptide immediately before Lys320 (Fig. 3A). We found, however, that this GS insertion abolished 14-3-3 binding to CDC25B, despite the fact that phosphorylation at site 309 was detected with phospho-Ser309 antibodies (Fig. 3B).

These results were intriguing because there have been no previous reports that amino acid sequences C-terminal

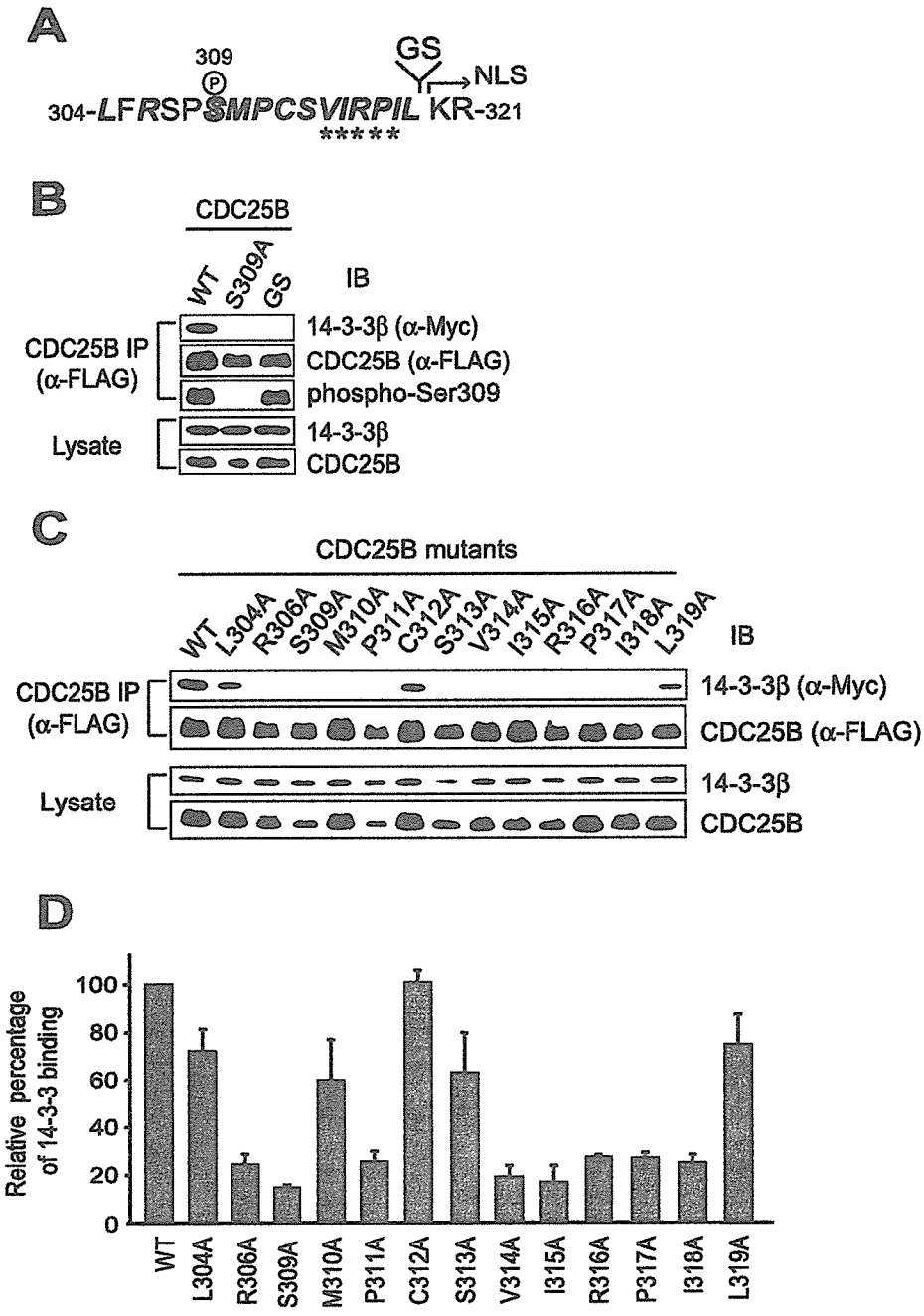

Fig. 3. **Binding of 14-3-3β to CDC25B mutants with substitutions near Ser309.** CDC25B mutants containing point substitutions near Ser309 were co-transfected with 14-3-3β, and CDC25B mutant proteins were isolated with anti-FLAG-agarose beads as described in Fig. 2. CDC25B-bound 14-3-3β was identified with an anti-myc antibody. A. Amino acid sequence from Leu304 to Arg321. Ser309 is denoted by an outlined letter S. A *Bam*HI site (GGATCC), which encodes Gly–Ser, was inserted between Leu319 and Lys320. Lys320 is the N-terminal end of the NLS sequence in CDC25B, which is indicated by an arrow. Bold italic letters indicate amino acids changed to Ala to analyze 14-3-3 binding, the results of which are depicted in (C) and (D). Asterisks indicate the hydrophobic amino acid stretch (see text). The GS insertion mutant (+ GS in B) and a series of point mutants (C) of CDC25B were analyzed as to their binding to 14-3-3β and the phosphorylation of Ser309, which was determined with anti-phospho-Ser309 antibodies. The efficiency of 14-3-3β binding to each CDC25B mutant relative to wild-type CDC25B was calculated from the data presented in (C) and is depicted in (D). The data shown are the averages of three independent experiments. Bars = standard deviation.

to the 14-3-3 binding site affect the interaction between 14-3-3 and its target proteins. We further examined this phenomenon by introducing single alanine point mutations at residues 304 to 319 of CDC25B, and then co-transfecting the resulting mutants and 14-3-3β (indicated by bold italic letters in Fig. 3A). Surprisingly, all of the tested point mutations except Cys312Ala and Leu319Ala caused a diminished interaction with 14-3-3 (Fig. 3C). The results clearly demonstrate that the hydrophobic amino acid region from Val315 to Ile318 seems to be important for 14-3-3 binding (Fig. 3D and depicted by asterisks in Fig. 3A). Pro311 of CDC25B, which is part of the 14-3-3 binding consensus sequence, also appeared to be important for 14-3-3 binding. Thus, alterations in the amino acids near the core consensus sequence of site 309 of CDC25B negatively affected its ability to bind to 14-3-3.

Ser309 Phosphorylation by Several Candidate Kinases—To study the *in vivo* phosphorylation of Ser309 in these mutants, we transfected some of the mutant *CDC25B* genes, and the mutant proteins were recovered and assayed for phosphorylation at Ser309. As shown in Fig. 4A, phosphorylation of Ser309 occurred in all of the mutants expressed in HEK293 cells, except for the Pro317Ala mutant expressed in Cos-7 cells.

Several kinases that phosphorylate Ser309 of CDC25B1 (or Ser323 of CDC25B3) have been reported. We attempted to determine which kinases could phosphorylate the CDC25B mutants. We expressed candidate kinases

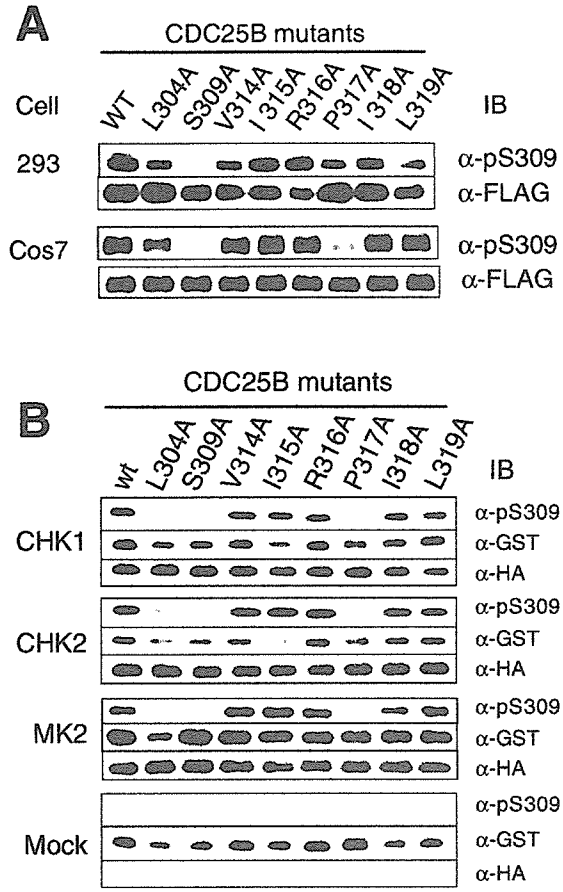

Fig. 4. **Phosphorylation of Ser309 *in vivo* and *in vitro* by representative kinases.** HEK293 cells (1.4×10^6 cells per 35-mm plate) or Cos-7 cells (2×10^5 cells per 35-mm plate) were transfected with plasmids carrying FLAG-tagged CDC25B mutants, and the expressed proteins were immunoprecipitated with monoclonal anti-FLAG beads. The precipitated proteins were immunoblotted with anti-FLAG or anti-phospho-Ser309 antibodies (A). His- and HA-tagged kinases were expressed in Cos-7 cells and recovered as described. The recovered kinases were incubated with GST-fused CDC25B peptides (wild-type or mutant), and phosphorylation at Ser309 was determined by immunoblotting (B).

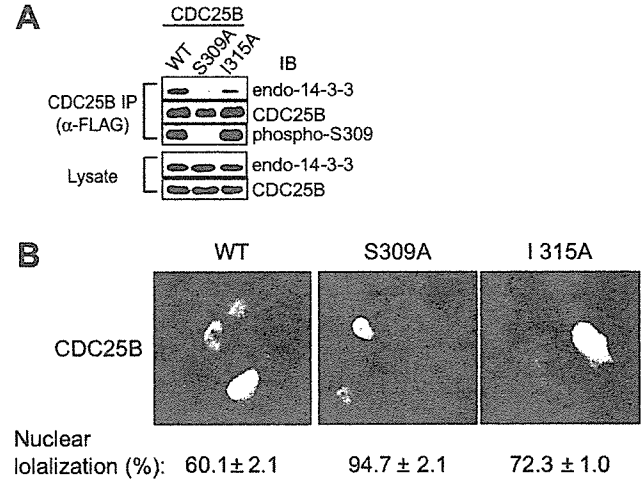

Fig. 5. **Binding of endogenous 14-3-3 to CDC25B mutants and subcellular localization.** HEK293 cells were transfected with plasmids carrying wild type CDC25B or Ala309 or Ala315 mutants, and the expressed proteins were recovered with anti-FLAG beads. The precipitates were immunoblotted with an anti-pan 14-3-3 antibody (upper panel), anti-FLAG antibody (second panel), or anti–phospho-Ser309 antibody (third panel). The expression of endogenous 14-3-3 and transfected CDC25B is indicated in the two bottom panels (A). HEK293 cells were transfected with CDC25B plasmids as in (A), and the subcellular localization of the expressed CDC25B proteins was determined as in Fig. 2D. The numbers represent the percentages of cells expressing the CDC25B protein found exclusively in the nucleus. Three independent experiments were performed for each value , and more than 200 CDC25B-expressing cells were counted in each experiment (B).

CHK1 (*18*), CHK2 (*19*) and MK2 (*26*) in Cos-7 cells and then recovered the kinases by immunoprecipitation. For the preparation of MK2, an upstream kinase, mitogen-activated protein kinase kinase kinase 6 (MKK6) and MK2 were co-transfected, and the expressed MK2 was immunoprecipitated. An *in vitro* phosphorylation assay indicated that the three kinases could phosphorylate GST-tagged CDC25B mutant peptides (Fig. 4B), the results being similar to those obtained *in vivo* (Fig. 4A). The kinases phosphorylated all of the mutant peptides with similar efficiency, with the exception of the Pro317Ala mutant, consistent with the results shown in Fig. 4A. These results demonstrate that Ser309 of CDC25B can be phosphorylated by several kinases.

Binding of Endogenous 14-3-3 to CDC25B Mutants and Their Subcellular Localization—We examined the binding of endogenous 14-3-3 to mutant CDC25B proteins. After transfection to HEK293 cells, CDC25B proteins were recovered, and the bound 14-3-3 protein was quantitated using a pan-14-3-3 antibody. Figure 5A shows that the efficiency of endogenous 14-3-3 binding to mutant CDC25B was similar to that in the co-expression experiments. Endogenous 14-3-3 bound to wild-type CDC25B most efficiently and to the 309Ala mutant least efficiently. A lesser amount of endogenous 14-3-3 was detected with the 315Ala mutant, which exactly matched the results in Fig. 3C and D. The phosphorylation of S309 in the I315A mutant could also be reproduced (compare Figs. 5A and 4A). We examined the subcellular localization of these mutant CDC25B proteins expressed in cells (Fig. 5B). The number of cells with CDC25B specifically localized in the nucleus was higher for mutant CDC25B than for the wild-type protein. About 72% of the cells exhibited specific nuclear localization of CDC25B 315Ala mutants, which was higher than the frequency of nuclear localization of wild-type CDC25B (~60%). Collectively, amino acid sequences surrounding the 14-3-3 binding core consensus site have a strong influence on 14-3-3 binding but subcellular localization of CDC25B can not be simply explained by 14-3-3 binding.

Finally, the results of this study are summarized in Table 3.

DISCUSSION

Seven isoforms of 14-3-3 have been identified in mammalian cells. We previously reported that three isoforms, 14-3-3β, ε, and σ, are able to bind to CDC25B, and that the

Table 3. **Summary of 14-3-3β binding and Ser309 phosphorylation of each CDC25B mutant.**

Name	Sequence	14-3-3β Binding (%)	Ser309 phosphorylation	
			in vivo	*in vitro*
WT	^{304}LFRSPSMPCSVIRPILKR^{321}	100	+	+
GS	LFRSPSMPCSVIRPILGSKR	17	+	NT
L304A	A- - - - - - - - - - - - - -KR	70	+	±
R306A	- -A- - - - - - - - - - - -KR	23	NT	NT
S309A	- - - - -A- - - - - - - - -KR	18	–	–
M310A	- - - - - -A- - - - - - - -KR	60	NT	NT
P311A	- - - - - - -A- - - - - - -KR	25	NT	NT
C312A	- - - - - - - -A- - - - - -KR	103	NT	NT
S313A	- - - - - - - - -A- - - - -KR	63	NT	NT
V314A	- - - - - - - - - -A- - - -KR	21	+	+
I315A	- - - - - - - - - - -A- - -KR	17	+	+
R316A	- - - - - - - - - - - -A- -KR	27	+	+
P317A	- - - - - - - - - - - - -A-KR	27	+	±
I318A	- - - - - - - - - - - - - -AKR	25	+	+
L319A	- - - - - - - - - - - - - -AKR	72	+	+

binding site for 14-3-3β and ε is different from that for 14-3-3σ. Moreover, after binding to 14-3-3β or ε but not σ, CDC25B is exported to the cytoplasm. The recently published X-ray structure results revealed the following specific functional and structural features of the 14-3-3σ isoform. First, it usually forms a homodimer. Second, 14-3-3σ possesses a ligand-discriminating, special amino acid patch on the second ligand-binding surface (*38*). These findings may explain the difference in the binding properties of 14-3-3β and σ as to CDC25B.

Here, we evaluated whether four other 14-3-3 subtypes (γ, η, θ/τ, and ζ) also bind to CDC25B and exhibit behavior similar to that of 14-3-3β. The 14-3-3θ/τ isoform exhibited slightly different properties from those of the other three isoforms in that it bound to other 14-3-3 motifs in CDC25B in addition to site 309. The 14-3-3ζ isoform bound to CDC25B more weakly at Ser309 than did the other isoforms, except 14-3-3σ. These subtle differences appeared to affect the ability of these isoforms to cause the transfer of CDC25B from the nucleus to the cytoplasm. Our results show that six of the seven 14-3-3 subtypes in mammalian cells behave similarly in terms of CDC25B binding. The specific function of the 14-3-3σ isoform is unknown.

The typical consensus 14-3-3 binding sequence consists of Arg-X-X-Ser/Thr-X-P (mode-I) or Arg-X-X-X-Ser/Thr-X-P (mode-II), where the serine or threonine must be phosphorylated (*39*, *40*). In addition to these binding motifs, 14-3-3 also binds to the recently identified mode-III motif, which consists of (p)S/T-X_{1-2}-COOH at the C-terminus of several proteins (*41*). Although the results of oriented peptide analysis suggest that the Arg-X-X-(p)Ser/Thr-X-P mode-I motif is sufficient for 14-3-3 binding, a more complicated situation appears to exist *in vivo*. For example, we previously found that CDC25B contains five 14-3-3 binding motifs, but only three of these are functional. The principal 14-3-3 binding site is at Ser309, and the Ser216 site in combination with the Ser137 or Ser309 site may also be important, especially for binding to 14-3-3σ.

One possible reason for the apparent non-functionality of certain 14-3-3 binding motifs *in vivo* may be the lack of phosphorylation of target Ser/Thr. The results described in this report suggest another somewhat unexpected explanation. We found that alterations in amino acids C-terminal to the binding motif at site 309 severely impaired 14-3-3 binding, indicating that 14-3-3 binding depends not only on the consensus sequence but also on its context. Thus, the binding of 14-3-3 may require not only the presence of the binding motif in its appropriately phosphorylated form but also the presence of a suitable sequence C-terminal to the binding site. Substitution mutations of amino acid residues often disrupt the local structure of proteins. Therefore, some mutants examined in this study may harbor a structural change that abolishes 14-3-3 binding. However, Ser309 in each CDC25B mutant, except Pro317Ala, was efficiently phosphorylated at the same level as that of the wild-type protein in transfected cells. These results imply (but do not prove unequivocally) that a gross structural change should not be introduced by the mutations. Studies using an oriented peptide library with a random amino acid sequence placed C-terminal to the consensus site will be important for confirmation of our hypothesis.

The specific kinases that phosphorylate Ser309 of CDC25B have yet to be identified. We examined kinases that have been reported to phosphorylate this residue, but they exhibited essentially the same specificity toward mutated substrates *in vitro*. All of the tested kinases required a proline at residue 317 and an arginine at residue 306, although Pro317 was not essential for Ser309 phosphorylation *in vivo*. The kinase responsible for regulating CDC25B localization must exhibit an appropriate subcellular localization. In the normal cell cycle, CDC25B is located in the nucleus, and Ser309 is phosphorylated to some degree even in the absence of cellular injury (*23*). In view of this, kinases that phosphorylate Ser309 would also be expected to be located in the nucleus. Of these kinases, we propose that CHK1 and MK2 may be suitable for the phosphorylation of Ser309 of CDC25B1, even in the absence of specific cellular damage, since they are activated at low levels during DNA replication and environmental stress, respectively (Ref. *26* and our unpublished data). It is a matter for further investigation

as to whether these kinases phosphorylate this site more heavily when cells are injured.

We thank S. Elledge for the generous gift of the plasmids. This work was supported by Grants-in-Aid for Scientific Research from and by the Third-Term Comprehensive 10-Year Strategy for Cancer Control of the Ministry of Health, Labour, and Welfare of Japan. This work was also supported by the Collaborative Research Program of the Cancer Institute of Kanazawa University and by the Kanazawa University 21st Century COE Program of the Ministry of Education, Culture, Sports, Science, and Technology of Japan. S. U. was also supported by a fellowship from the Kanazawa University 21st Century COE Program and a Research-Resident Fellowship from the Human Science Foundation of Japan.

REFERENCES

1. Galaktionov, K. and Beach, D. (1991) Specific activation of cdc25 tyrosine phosphatases by B-type cyclins: evidence for multiple roles of mitotic cyclins. *Cell* **67**, 1181–1194
2. Sadhu, K., Reed, S.I., Richardson, H., and Russell, P. (1990) Human homolog of fission yeast cdc25 mitotic inducer is predominantly expressed in G2. *Proc. Natl. Acad. Sci. USA* **87**, 5139–5143
3. Strausfeld, U., Labbe, J.C., Fesquet, D., Cavadore, J.C., Picard, A., Sadhu, K., Russell, P., and Doree, M. (1991) Dephosphorylation and activation of a p34cdc2/cyclin B complex in vitro by human CDC25 protein. *Nature* **351**, 242–245
4. Jinno, S., Suto, K., Nagata, A., Igarashi, M., Kanaoka, Y., Nojima, H., and Okayama, H. (1994) Cdc25A is a novel phosphatase functioning early in the cell cycle. *EMBO J.* **13**, 1549–1556
5. Hoffmann, I., Draetta, G., and Karsenti, E. (1994) Activation of the phosphatase activity of human cdc25A by a cdk2-cyclin E dependent phosphorylation at the G1/S transition. *EMBO J.* **13**, 4302–4310
6. Kumagai, A. and Dunphy, W.G. (1992) Regulation of the cdc25 protein during the cell cycle in Xenopus extracts. *Cell* **70**, 139–151
7. Hoffmann, I., Clarke, P.R., Marcote, M.J., Karsenti, E., and Draetta, G. (1993) Phosphorylation and activation of human cdc25-C by cdc2—cyclin B and its involvement in the self-amplification of MPF at mitosis. *EMBO J.* **12**, 53–63
8. Nishijima, H., Nishitani, H., Seki, T., and Nishimoto, T. (1997) A dual-specificity phosphatase Cdc25B is an unstable protein and triggers p34(cdc2)/cyclin B activation in hamster BHK21 cells arrested with hydroxyurea. *J. Cell Biol.* **138**, 1105–1116
9. Lammer, C., Wagerer, S., Saffrich, R., Mertens, D., Ansorge, W., and Hoffmann, I. (1998) The cdc25B phosphatase is essential for the G2/M phase transition in human cells. *J. Cell Sci.* **111**, 2445–2453
10. Donzelli, M., Squatrito, M., Ganoth, D., Hershko, A., Pagano, M., and Draetta, G.F. (2002) Dual mode of degradation of Cdc25 A phosphatase. *EMBO J.* **21**, 4875–4884
11. Mailand, N., Podtelejnikov, A.V., Groth, A., Mann, M., Bartek, J., and Lukas, J. (2002) Regulation of G(2)/M events by Cdc25A through phosphorylation-dependent modulation of its stability. *EMBO J.* **21**, 5911–5920
12. Chen, M.S., Hurov, J., White, L.S., Woodford-Thomas, T., and Piwnica-Worms, H. (2001) Absence of apparent phenotype in mice lacking Cdc25C protein phosphatase. *Mol. Cell. Biol.* **21**, 3853–3861
13. Lincoln, A.J., Wickramasinghe, D., Stein, P., Schultz, R.M., Palko, M.E., De Miguel, M.P., Tessarollo, L., and Donovan, P.J. (2002) Cdc25b phosphatase is required for resumption of meiosis during oocyte maturation. *Nat. Genet.* **30**, 446–449
14. Ferguson, A.M., White, L.S., Donovan, P.J., and Piwnica-Worms, H. (2005) Normal cell cycle and checkpoint responses in mice and cells lacking Cdc25B and Cdc25C protein phosphatases. *Mol. Cell. Biol.* **25**, 2853–2860
15. Bulavin, D.V., Amundson, S.A., and Fornace, A.J. (2002) p38 and Chk1 kinases: different conductors for the G(2)/M checkpoint symphony. *Curr. Opin. Genet. Dev.* **12**, 92–97
16. Donzelli, M. and Draetta, G.F. (2003) Regulating mammalian checkpoints through Cdc25 inactivation *EMBO Rep.* **4**, 671–677
17. Bartek, J., Lukas, C., and Lukas, J. (2004) Checking on DNA damage in S phase. *Nat. Rev. Mol. Cell. Biol.* **5**, 792–804
18. Sanchez, Y., Wong, C., Thoma, R.S., Richman, R., Wu, Z., Piwnica-Worms, H., and Elledge, S.J. (1997) Conservation of the Chk1 checkpoint pathway in mammals: linkage of DNA damage to Cdk regulation through Cdc25. *Science* **277**, 1497–1501
19. Matsuoka, S., Huang, M., and Elledge, S.J. (1998) Linkage of ATM to cell cycle regulation by the Chk2 protein kinase. *Science* **282**, 1893–1897
20. O'Neill, T., Giarratani, L., Chen, P., Iyer, L., Lee, C.H., Bobiak, M., Kanai, F., Zhou, B.B., Chung, J.H., and Rathbun, G.A. (2002) Determination of substrate motifs for human Chk1 and hCds1/Chk2 by the oriented peptide library approach. *J. Biol. Chem.* **277**, 16102–16115
21. Miyata, H., Doki, Y., Yamamoto, H., Kishi, K., Takemoto, H., Fujiwara, Y., Yasuda, T., Yano, M., Inoue, M., Shiozaki, H., Weinstein, I.B., and Monden, M. (2001) Overexpression of CDC25B overrides radiation-induced G2-M arrest and results in increased apoptosis in esophageal cancer cells. *Cancer Res.* **61**, 3188–3193
22. Forrest, A. and Gabrielli, B. (2001) Cdc25B activity is regulated by 14-3-3. *Oncogene* **20**, 4393–4401
23. Bulavin, D.V., Higashimoto, Y., Popoff, I.J., Gaarde, W.A., Basrur, V., Potapova, O., Appella, E., and Fornace, A.J., Jr. (2001) Initiation of a G2/M checkpoint after ultraviolet radiation requires p38 kinase. *Nature* **411**, 102–107
24. Peng, C.Y., Graves, P.R., Thoma, R.S., Wu, Z., Shaw, A.S., and Piwnica-Worms, H. (1997) Mitotic and G2 checkpoint control: regulation of 14-3-3 protein binding by phosphorylation of Cdc25C on serine-216. *Science* **277**, 1501–1505
25. Giles, N., Forrest, A., and Gabrielli, B. (2003) 14-3-3 acts as an intramolecular bridge to regulate cdc25B localization and activity. *J. Biol. Chem.* **278**, 28580–28587
26. Manke, I.A., Nguyen, A., Lim, D., Stewart, M.Q., Elia, A.E., and Yaffe, M.B. (2005) MAPKAP kinase-2 is a cell cycle checkpoint kinase that regulates the G2/M transition and S phase progression in response to UV irradiation. *Mol. Cell* **17**, 37–48
27. Dalal, S.N., Schweitzer, C.M., Gan, J., and DeCaprio, J.A. (1999) Cytoplasmic localization of human cdc25C during interphase requires an intact 14-3-3 binding site. *Mol. Cell. Biol.* **19**, 4465–4479
28. Davezac, N., Baldin, V., Gabrielli, B., Forrest, A., Theis-Febvre, N., Yashida, M., and Ducommun, B. (2000) Regulation of CDC25B phosphatases subcellular localization. *Oncogene* **19**, 2179–2185
29. Graves, P.R., Lovly, C.M., Uy, G.L., and Piwnica-Worms, H. (2001) Localization of human Cdc25C is regulated both by nuclear export and 14-3-3 protein binding. *Oncogene* **20**, 1839–1851
30. Uchida, S., Kuma, A., Ohtsubo, M., Shimura, M., Hirata, M., Nakagama, H., Matsunaga, T., Ishizaka, Y., and Yamashita, K. (2004) Binding of 14-3-3beta but not 14-3-3sigma controls the cytoplasmic localization of CDC25B: binding site preferences of 14-3-3 subtypes and the subcellular localization of CDC25B. *J. Cell Sci.* **117**, 3011–3020
31. Furnari, B., Blasina, A., Boddy, M.N., McGowan, C.H., and Russell, P. (1999) Cdc25 inhibited in vivo and in vitro by checkpoint kinases Cds1 and Chk1. *Mol. Biol. Cell* **10**, 833–845

32. Chen, M.S., Ryan, C.E., and Piwnica-Worms, H. (2003) Chk1 kinase negatively regulates mitotic function of Cdc25A phosphatase through 14-3-3 binding. *Mol. Cell. Biol.* **23**, 7488–7497
33. Uto, K., Inoue, D., Shimuta, K., Nakajo, N., and Sagata, N. (2004) Chk1, but not Chk2, inhibits Cdc25 phosphatases by a novel common mechanism. *EMBO J.* **23**, 3386–3396
34. Guan, K.L. and Dixon, J.E. (1991) Eukaryotic proteins expressed in Escherichia coli: an improved thrombin cleavage and purification procedure of fusion proteins with glutathione S-transferase. *Anal. Biochem.* **192**, 262–267
35. Wang, X., Arooz, T., Siu, W.Y., Chiu, C.H., Lau, A., Yamashita, K., and Poon, R.Y. (2001) MDM2 and MDMX can interact differently with ARF and members of the p53 family. *FEBS Lett.* **490**, 202–208
36. Bradford, M.M. (1976) A rapid and sensitive method for the quantitation of microgram quantities of protein utilizing the principle of protein-dye binding. *Anal. Biochem.* **72**, 248–254
37. Uchida, S., Ohtsubo, M., Shimura, M., Hirata, M., Nakagama, H., Matsunaga, T., Yoshida, M., Ishizaka, Y., and Yamashita, K. (2004) Nuclear export signal in CDC25B. *Biochem. Biophys. Res. Commun.* **316**, 226–232
38. Wilker, E.W., Grant, R.A., Artim, S.C., and Yaffe, M.B. (2005) A structural basis for 14-3-3sigma functional specificity. *J. Biol. Chem.* **280**, 18891–18898
39. Muslin, A.J., Tanner, J.W., Allen, P.M., and Shaw, A.S. (1996) Interaction of 14-3-3 with signaling proteins is mediated by the recognition of phosphoserine. *Cell* **84**, 889–897
40. Yaffe, M.B., Rittinger, K., Volinia, S., Caron, P.R., Aitken, A., Leffers, H., Gamblin, S.J., Smerdon, S.J., and Cantley, L.C. (1997) The structural basis for 14-3-3:phosphopeptide binding specificity. *Cell* **91**, 961–971
41. Ganguly, S., Weller, J.L., Ho, A., Chemineau, P., Malpaux, B., and Klein, D.C. (2005) Melatonin synthesis: 14-3-3-dependent activation and inhibition of arylalkylamine N-acetyltransferase mediated by phosphoserine-205. *Proc. Natl. Acad. Sci. USA* **102**, 1222–1227